

Universität des Saarlandes



Fachrichtung 6.1 – Mathematik

Preprint Nr. 283

**Residual error estimate for BEM-based FEM on
polygonal meshes**

Steffen Weißer

Saarbrücken 2010

Residual error estimate for BEM-based FEM on polygonal meshes

Steffen Weißer

Saarland University
Department of Mathematics
P.O. Box 15 11 50
66041 Saarbrücken
Germany
`weisser@num.uni-sb.de`

Edited by
FR 6.1 – Mathematik
Universität des Saarlandes
Postfach 15 11 50
66041 Saarbrücken
Germany

Fax: + 49 681 302 4443
e-Mail: preprint@math.uni-sb.de
WWW: <http://www.math.uni-sb.de/>

Residual error estimate for BEM-based FEM on polygonal meshes

Steffen Weißer

March 2, 2011

Abstract

A conforming finite element method on polygonal meshes is reviewed which handles hanging nodes naturally. Trial functions are defined to fulfil the homogeneous PDE locally and they are treated by means of local boundary integral equations. Using a quasi-interpolation operator of Clément type a residual-based error estimate is obtained. This a posteriori estimator can be used to rate the accuracy of the approximation over polygonal elements or it can be applied to an adaptive BEM-based FEM. The numerical experiments confirm our results and show optimal convergence for the adaptive strategy on general meshes.

Keywords non-standard finite element method · a posteriori error estimate · adaptivity · polygonal/polyhedral mesh

Mathematics Subject Classification (2000) 65N15 · 65N30 · 65N38 · 65N50

1 Introduction

The interest in more flexible and general meshes for the numerical approximation of boundary value problems has been increased. Brezzi, Lipnikov and Shashkov published convergence results for the mimetic finite difference method on polyhedral meshes [4]. Other authors like Dolejší, Feistauer and Sobotíková analysed the discontinuous Galerkin method on such meshes [9]. In recent years, residual error estimates have been invented for these two methods and their variations [2, 3]. This increased interest shows the need for advanced methods which handle general meshes.

In contrast to the non-conforming mimetic finite difference method and the discontinuous Galerkin method, we review a conforming finite element method with local PDE-harmonic trial functions. This BEM-based finite element method was first proposed by Copeland, Langer and Pusch [7] in 2009. Copeland additionally discussed the method for Helmholtz and Maxwell equations in [8] and a rigorous

error analysis was performed by Hofreither, Langer and Pechstein [11]. Local boundary integral formulations as well as boundary element methods (BEM) in the numerics are used to treat the implicitly defined trial functions.

In the following section, we introduce the stationary isotropic heat equation and its variational formulation as a model problem. Additionally, we state the regularity assumptions on a polygonal mesh and give some notations as well as a short introduction into boundary integral formulations. Afterwards, in the third section, the BEM-based finite element method is described.

In section four, we list a few properties of regular polygonal meshes, use them to introduce a quasi-interpolation operator and prove approximation estimates with the help of [17]. Using this operator in section five, the reliability of a residual-based error estimator is proven in the style of Verfürth [18]. This a posteriori error estimate allows to rate the accuracy of the approximation over polygonal elements.

The numerical examples at the end confirm our results and show optimal rates of convergence for an adaptive finite element strategy on polygonal meshes. Finally, we discuss a special property of refined meshes for the adaptive BEM-based FEM and give some conclusions.

2 Preliminaries

We choose a model problem to study the special finite element method, namely the stationary heat equation with isotropic material properties. Let $\Omega \subset \mathbb{R}^2$ be a bounded polygonal Lipschitz domain with boundary $\Gamma = \Gamma_D \cup \Gamma_N$ and $|\Gamma_D| > 0$. The boundary value problem reads

$$\begin{aligned} -\operatorname{div}(a(x)\nabla u(x)) &= f(x) && \text{for } x \in \Omega, \\ u(x) &= g_D(x) && \text{for } x \in \Gamma_D, \\ a(x)\nabla u(x) \cdot n(x) &= g_N(x) && \text{for } x \in \Gamma_N, \end{aligned} \tag{1}$$

where $f \in L_2(\Omega)$, $g_D \in H^{1/2}(\Gamma_D)$, $g_N \in L_2(\Gamma_N)$, n the outer normal vector of Ω and $a \in L_\infty(\Omega)$ piecewise constant with $0 < a_{\min} \leq a(x) \leq a_{\max}$ for $x \in \Omega$. The properties of a ensure the coercivity of the problem. Since $g_D \in H^{1/2}(\Gamma_D)$, an extension u_D of g_D exists with $u_D \in H^1(\Omega)$.

In contrast to [7, 11], we are dealing with mixed boundary conditions and we do not simplify the problem to end up with the Laplace equation as in [11]. Let $V = H_D^1(\Omega) = \{v \in H^1(\Omega) : \gamma_0 v = 0 \text{ on } \Gamma_D\}$ and $u_D + V = \{u_D + v : v \in V\}$, where $\gamma_0 : H^1(\Omega) \rightarrow H^{1/2}(\Gamma)$ is the trace on Γ defined in [1]. Then we obtain the variational formulation

$$\text{Find } u \in u_D + V : \quad a_\Omega(u, v) = (f, v) + (g_N, v)_{\Gamma_N}, \quad \forall v \in V$$

with the L_2 -scalar products (\cdot, \cdot) and $(\cdot, \cdot)_{\Gamma_N}$ over Ω and Γ_N , respectively, and the bilinear form

$$a_{\Omega}(u, v) = \int_{\Omega} a(x) \nabla u(x) \cdot \nabla v(x) dx.$$

Using the representation $u = u_D + u_0$, $u_0 \in V$, we rewrite the formulation

$$\text{Find } u_0 \in V : \quad a_{\Omega}(u_0, v) = (f, v) + (g_N, v)_{\Gamma_N} - a_{\Omega}(u_D, v), \quad \forall v \in V.$$

The bilinear form $a_{\Omega}(\cdot, \cdot)$ is bounded and coercive on V . Therefore, the problem has a unique solution according to the Lax-Milgram theorem.

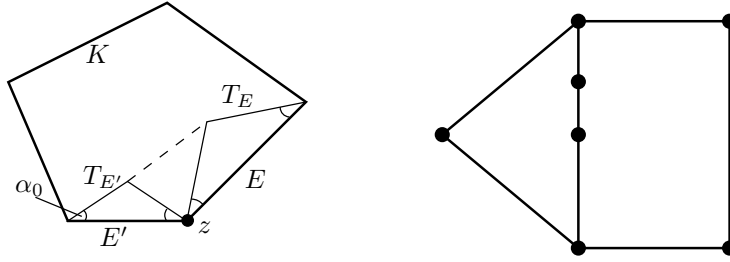


Figure 1: Element with two isosceles triangles adjacent to the node z (left), triangle and rectangle which are turned to polygons (right)

For the numeric, we have to introduce a discretization \mathcal{K}_h of the domain Ω . We allow polygonal meshes which are a generalisation of standard triangulations as well as of quadrilateral meshes. The compact polygonal elements $K \in \mathcal{K}_h$ are non-overlapping. In every corner of an element is a node, but it is also possible, that there are more nodes on the boundary of each element, see Figure 1. We stress this fact more carefully. If we have a triangle with three nodes and we add some nodes on the boundary, this triangle turns formally into a polygon. These additional nodes will enrich the approximation space in the finite element method in section 3. In this context, hanging nodes appear naturally since they are just classical nodes for polygons. An edge is always located between two nodes and the intersection of two edges is either empty or a node. It is not allowed that an edge contains more than two nodes, the start and the end point. We have

$$\bar{\Omega} = \bigcup_{K \in \mathcal{K}_h} K.$$

The diameter of an element $K \in \mathcal{K}_h$ and the length of an edge E are denoted by h_K and h_E , respectively.

Definition 1. The mesh \mathcal{K}_h is called regular if it fulfils:

1. There is an angle α_0 with $0 < \alpha_0 \leq \pi/3$ such that for all elements $K \in \mathcal{K}_h$ and all its edges $E \subset \partial K$ the isosceles triangle with longest side E and two interior angles α_0 lies inside the element K . This triangle is labelled T_E , see Figure 1.

2. There is a constant $c_1 > 0$ such that for all elements $K \in \mathcal{K}_h$ and all its edges $E \subset \partial K$ we have $h_K \leq c_1 h_E$.
3. All elements $K \in \mathcal{K}_h$ are convex.

The first condition ensures that the interior angles of the polygonal elements are bounded away from zero and that the elements do not get too thin. This condition is more restrictive than the inner cone condition, since it additionally bounds the thickness of the elements from below. The second condition says that the length of an edge of an element is not too small compared with the size of the element. In the case that we deal with a sequence of meshes, for example in adaptive strategies, the conditions have to hold uniformly for all $h > 0$.

Additionally, we assume in the following that $h_K < 1$ for all elements $K \in \mathcal{K}_h$. This condition is no grievous restriction on the mesh, since $h_K < 1$ can always be satisfied by scaling Ω . Nevertheless, it is needed for the local boundary integral formulations.

We need some more notation. \mathcal{N}_h is the set of all nodes in the mesh \mathcal{K}_h . It is $\mathcal{N}_h = \mathcal{N}_{h,\Omega} \cup \mathcal{N}_{h,D} \cup \mathcal{N}_{h,N}$ where $\mathcal{N}_{h,\Omega}$, $\mathcal{N}_{h,D}$, $\mathcal{N}_{h,N}$ contain the nodes in the interior of Ω , on the Dirichlet boundary Γ_D and on the interior of the Neumann boundary Γ_N , respectively. We label the set of all edges of the mesh with \mathcal{E}_h . Moreover, the sets $\mathcal{N}(K)$ and $\mathcal{N}(E)$ contain all nodes which belong to the element $K \in \mathcal{K}_h$ and the edge $E \in \mathcal{E}_h$, respectively. Since elements are compact subdomains of Ω , we label the interior of an element $K \in \mathcal{K}_h$ with $\overset{\circ}{K}$.

In the following we assume that the coefficient a is constant on each element $K \in \mathcal{K}_h$ and we write $a(x) = a_K$ for $x \in K$.

In the remainder of this section, we introduce some expressions from the theory of boundary integral formulations. We focus on the partial differential equation of our model problem on each element $K \in \mathcal{K}_h$. Since the coefficient a is constant on each element, it can be taken out of the divergence expression. This yields the Poisson equation

$$-\Delta u = f/a_K \quad \text{on } \overset{\circ}{K}.$$

For the following theory of boundary integral formulations, we need the usual trace operator $\gamma_0^K : H^1(\overset{\circ}{K}) \rightarrow H^{1/2}(\partial K)$ which is defined in [1], for example. Let $v \in H^1(\overset{\circ}{K})$ with Δv in the dual of $H^1(\overset{\circ}{K})$. Due to Green's first identity [12], there exists a unique function $\gamma_1^K v \in H^{-1/2}(\partial K)$ such that

$$\int_{\overset{\circ}{K}} \nabla v(y) \cdot \nabla w(y) dy = \int_{\partial K} \gamma_1^K v(y) \gamma_0^K w(y) ds_y - \int_{\overset{\circ}{K}} w(y) \Delta v(y) dy$$

for $w \in H^1(\overset{\circ}{K})$. We call $\gamma_1^K v$ the conormal derivative of v . If v is smooth, e.g. $v \in H^2(\overset{\circ}{K})$, we have

$$(\gamma_1^K v)(x) = n_K(x) \cdot (\gamma_0^K \nabla v)(x) \quad \text{for } x \in \partial K,$$

where $n_K(x)$ denotes the outer normal vector of the element K at x . The trace and the conormal derivative are also called Dirichlet and Neumann trace for the Laplace equation. The correct Neumann trace for the original equation (1) on ∂K is $a_K \gamma_1^K u$.

Additionally, we need the fundamental solution of the Laplacian. This singular function is given as

$$U^*(x, y) = -\frac{1}{2\pi} \ln |x - y| \quad \text{for } x, y \in \mathbb{R}^2.$$

The fundamental solution fulfils the equation

$$-\Delta_y U^*(x, y) = \delta_0(y - x),$$

where δ_0 is the Dirac delta distribution. If we substitute $v(y) = U^*(x, y)$ in Green's second identity

$$\int_K (v(y)\Delta u(y) - u(y)\Delta v(y)) dy = \int_{\partial K} (\gamma_0^K v(y)\gamma_1^K u(y) - \gamma_0^K u(y)\gamma_1^K v(y)) ds_y,$$

we obtain a representation formula for the solution u in every point $x \in \overset{\circ}{K}$. It reads

$$u(x) = \int_{\partial K} U^*(x, y)\gamma_1^K u(y) ds_y - \int_{\partial K} \gamma_{1,y}^K U^*(x, y)\gamma_0^K u(y) ds_y + \int_K U^*(x, y)\frac{f(y)}{a_K} dy.$$

The boundary functions $\gamma_0^K u$ and $\gamma_1^K u$ are called Dirichlet data and Neumann data, respectively. If this boundary data is known, it is possible to evaluate the function u everywhere in the element $\overset{\circ}{K}$. Furthermore, it is possible to evaluate the Neumann data if the Dirichlet data is known. We apply the trace operator and the conormal derivative operator to the representation formula. This yields the system of equations

$$\begin{pmatrix} \gamma_0^K u \\ \gamma_1^K u \end{pmatrix} = \begin{pmatrix} \frac{1}{2}\mathbf{I} - \mathbf{K}_K & \mathbf{V}_K \\ \mathbf{D}_K & \frac{1}{2}\mathbf{I} + \mathbf{K}'_K \end{pmatrix} \begin{pmatrix} \gamma_0^K u \\ \gamma_1^K u \end{pmatrix} + \begin{pmatrix} \mathbf{N}_{K,0}f/a_K \\ \mathbf{N}_{K,1}f/a_K \end{pmatrix}. \quad (2)$$

The system contains the standard boundary integral operators which are well studied, see e.g. [12, 16]. For $x \in \partial K$, we have the single-layer potential operator

$$(\mathbf{V}_K \zeta)(x) = \gamma_0^K \int_{\partial K} U^*(x, y)\zeta(y) ds_y \quad \text{for } \zeta \in H^{-1/2}(\partial K),$$

the double-layer potential operator

$$(\mathbf{K}_K \xi)(x) = \lim_{\varepsilon \rightarrow 0} \int_{y \in \partial K: |y-x| \geq \varepsilon} \gamma_{1,y}^K U^*(x, y)\xi(y) ds_y \quad \text{for } \xi \in H^{1/2}(\partial K),$$

and the adjoint double-layer potential

$$(\mathbf{K}'_K \zeta)(x) = \lim_{\varepsilon \rightarrow 0} \int_{y \in \partial K: |y-x| \geq \varepsilon} \gamma_{1,x}^K U^*(x, y) \zeta(y) ds_y \quad \text{for } \zeta \in H^{-1/2}(\partial K),$$

as well as the hypersingular integral operator

$$(\mathbf{D}_K \xi)(x) = -\gamma_1^K \int_{\partial K} \gamma_{1,y}^K U^*(x, y) \xi(y) ds_y \quad \text{for } \xi \in H^{1/2}(\partial K).$$

In addition, we have the Newton potential

$$(\mathbf{N}_{K,0} f)(x) = \gamma_0^K \int_K U^*(x, y) f(y) dy \quad \text{for } f \in H^{-1}(\overset{\circ}{K})$$

and its conormal derivative,

$$(\mathbf{N}_{K,1} f)(x) = \gamma_1^K \int_K U^*(x, y) f(y) dy \quad \text{for } f \in H^{-1}(\overset{\circ}{K})$$

for $x \in \partial K$. Since the diameter of K is smaller than one, the single-layer potential operator is invertible. Assuming f is identical to zero, the system (2) of boundary equations yields

$$\gamma_1^K u = \mathbf{S}_K \gamma_0^K u \quad \text{with} \quad \mathbf{S}_K = \mathbf{V}_K^{-1} \left(\frac{1}{2} \mathbf{I} + \mathbf{K}_K \right).$$

Therefore, we obtain the Dirichlet-to-Neumann map

$$a_K \gamma_1^K u = a_K \mathbf{S}_K \gamma_0^K u - \mathbf{V}_K^{-1} \mathbf{N}_{K,0} f \quad \text{on } \partial K.$$

The introduced operator \mathbf{S}_K is called Steklov-Poincaré operator. It has also a symmetric representation

$$\mathbf{S}_K = \mathbf{D}_K + \left(\frac{1}{2} \mathbf{I} + \mathbf{K}'_K \right) \mathbf{V}_K^{-1} \left(\frac{1}{2} \mathbf{I} + \mathbf{K}_K \right).$$

For the numerical implementation, the operator \mathbf{S}_K has to be approximated for all $K \in \mathcal{K}_h$ which leads to small local problems. We use standard boundary element method techniques as in [16]. For each element $K \in \mathcal{K}_h$, we choose the unrefined polygonal boundary as discretization of the boundary ∂K . Dirichlet traces are approximated by piecewise linear functions on the boundary which are continuous on ∂K . Functions in $H^{-1/2}(\partial K)$ are approximated by piecewise constant functions. Finally, we use a Galerkin scheme for the computation of the local boundary element matrices and obtain a discrete version

$$\mathbf{S}_{K,h} = \mathbf{D}_{K,h} + \left(\frac{1}{2} \mathbf{M}_{K,h}^\top + \mathbf{K}_{K,h}^\top \right) \mathbf{V}_{K,h}^{-1} \left(\frac{1}{2} \mathbf{M}_{K,h} + \mathbf{K}_{K,h} \right) \quad (3)$$

of the Steklov-Poincaré operator, see e.g. [16].

3 BEM-based finite element method

The authors who describe the BEM-based FEM in [8, 7, 11] rewrite the variational formulation of the model problem to get a formulation on the so called skeleton of the domain. This skeleton is as usual the union of all edges of the mesh. Afterwards, they approximate the trace of the solution on the skeleton and extend it to the domain. In contrast to these ideas, we follow the standard steps of a finite element method and reach finally the same system of linear equations. The finite element method needs some finite dimensional trial spaces

$$S_h(\Omega) \subset H^1(\Omega) \quad \text{and} \quad S_{Dh}(\Omega) \subset H_D^1(\Omega).$$

Therefore, we use

$$S_h(\Omega) = \text{span}\{\psi_z : z \in \mathcal{N}_h\} \quad \text{and} \quad S_{Dh}(\Omega) = \text{span}\{\psi_z : z \in \mathcal{N}_h \setminus \mathcal{N}_{h,D}\}.$$

For every node $z \in \mathcal{N}_h$, we define the trial function ψ_z as follows

$$\psi_z(x) = \begin{cases} 1 & \text{for } x = z \\ 0 & \text{for } x \in \mathcal{N}_h \setminus \{z\} \end{cases},$$

$$\psi_z \text{ is linear on each edge of the mesh,} \tag{4}$$

$$\Delta\psi_z = 0 \quad \text{in } \overset{\circ}{K} \quad \text{for all } K \in \mathcal{K}_h.$$

The trial functions are defined implicitly as solutions of local boundary value problems, see Figure 2. They are continuous, i.e. $\psi_z \in C(\overline{\Omega})$, and they are arbitrarily smooth in the interior of every element $K \in \mathcal{K}_h$, see e.g. [20]. Especially, we have $\psi_z \in C^2(\overset{\circ}{K})$ for $K \in \mathcal{K}_h$.

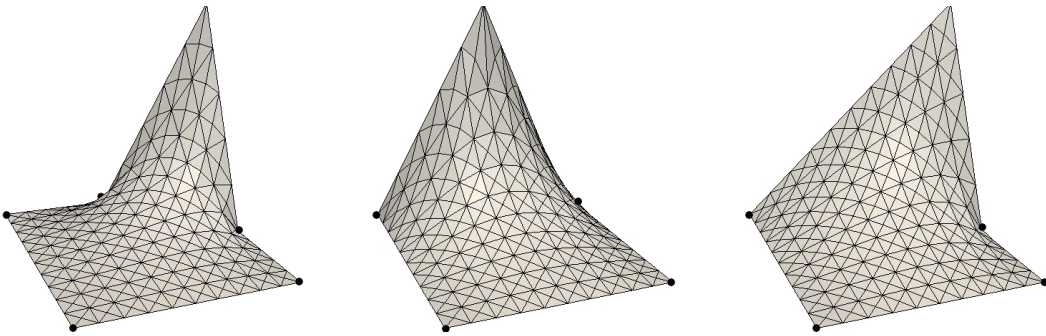


Figure 2: Trial functions on quadrangle elements with hanging nodes

On the well known elements of triangular and quadrilateral meshes, the trial functions are exactly the hat functions and the bilinear trial functions, respectively. This can be easily seen, since these classical trial functions fulfil the local boundary value problems (4) with unique solutions.

We approximate the exact boundary data g_D with a function g_{Dh} which is piecewise linear on the polygonal boundary Γ_D . Additionally, we choose an extension u_{Dh} of g_{Dh} in $S_h(\Omega)$. Let $V_h = S_{Dh}(\Omega) \subset V$. We obtain the Galerkin-formulation

$$\text{Find } u_{0h} \in V_h : \quad a_\Omega(u_{0h}, v_h) = (f, v_h) + (g_N, v_h)_{\Gamma_N} - a_\Omega(u_{Dh}, v_h), \quad \forall v_h \in V_h.$$

Unfortunately, it is difficult to integrate the implicitly defined functions ψ_z out of V_h and their gradients over the interior of the elements. For this reason, we use the theory of boundary integral operators to reformulate the given problem. Some easy computations show that the Galerkin-formulation, which is given above, is equivalent to

$$\text{Find } u_{0h} \in V_h : \quad a_\Omega^H(u_{0h}, v_h) = Lv_h - a_\Omega^H(u_{Dh}, v_h), \quad \forall v_h \in V_h,$$

with

$$a_\Omega^H(u, v) = \sum_{K \in \mathcal{K}_h} \int_{\partial K} a_K (\mathbf{S}_K \gamma_0^K u)(x) \gamma_0^K v(x) ds_x,$$

and

$$Lv = (g_N, v)_{\Gamma_N} + \sum_{K \in \mathcal{K}_h} \int_{\partial K} a_K (\mathbf{V}_K^{-1} \mathbf{N}_{K,0} f)(x) \gamma_0^K v(x) ds_x.$$

The discrete extension u_{Dh} of g_{Dh} can be chosen in such a way that it vanishes at every node in the interior of the domain Ω as well as at every node in the interior of the Neumann boundary Γ_N . The ansatz

$$u_{0h}(x) = \sum_{z \in \mathcal{N}_h \setminus \mathcal{N}_{h,D}} \alpha_z \psi_z(x) \quad \text{and} \quad u_{Dh}(x) = \sum_{z \in \mathcal{N}_{h,D}} \beta_z \psi_z(x)$$

yields a system of linear equations

$$\sum_{z \in \mathcal{N}_h \setminus \mathcal{N}_{h,D}} \alpha_z a_\Omega^H(\psi_z, \psi_x) = L\psi_x - \sum_{z \in \mathcal{N}_{h,D}} \beta_z a_\Omega^H(\psi_z, \psi_x), \quad \forall x \in \mathcal{N}_h \setminus \mathcal{N}_{h,D}$$

to determine the unknowns α_z . The coefficients β_z of u_{Dh} can be computed with interpolation or projection, for example. The advantage of this formulation is, that the implicitly defined trial functions are only evaluated on the boundaries of the elements where their Dirichlet traces are given explicitly and their Neumann traces can be computed by the use of the Steklov-Poincaré operator.

4 Quasi-interpolation operator

Before we can present the quasi-interpolation operator, we have to introduce some neighbourhoods of nodes, edges and elements. They are defined by

$$\omega_z = \bigcup_{z \in K'} K', \quad \omega_E = \bigcup_{E \cap K' \neq \emptyset} K', \quad \omega_K = \bigcup_{K \cap K' \neq \emptyset} K'$$

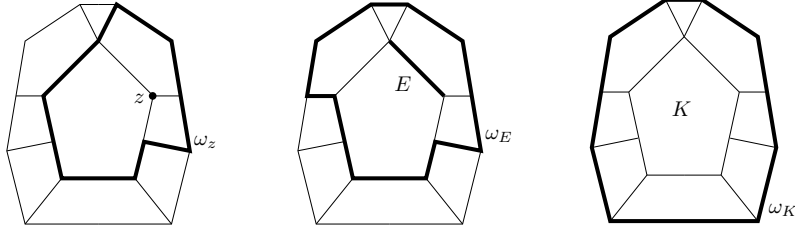


Figure 3: Examples for neighbourhoods of nodes, edges and elements

for $z \in \mathcal{N}_h$, $E \in \mathcal{E}_h$ and $K \in \mathcal{K}_h$, see also Figure 3. Let $Q_z : L_2(\omega_z) \rightarrow \mathbb{R}$ be the L_2 -projection into the space of constants. For $v \in H_D^1(\Omega)$, the quasi-interpolation operator $\mathfrak{I}_h : H_D^1(\Omega) \rightarrow S_{Dh}(\Omega)$ is defined by

$$\mathfrak{I}_h v = \sum_{z \in \mathcal{N}_h \setminus \mathcal{N}_{h,D}} (Q_z v) \psi_z.$$

The definition is very similar to the one of Clément [6]. The major difference is the use of non-polynomial trial functions on polygonal meshes. Our main interest in this section is to prove approximation properties of \mathfrak{I}_h in Proposition 1 below and to show a few properties of meshes that are regular in the sense of Definition 1. If no confusion can arise, we write v for both the function and the trace of the function on an edge.

Proposition 1. *Let \mathcal{K}_h be a regular mesh and let $v \in H_D^1(\Omega)$, $E \in \mathcal{E}_h$ and $K \in \mathcal{K}_h$. Then we have*

$$\begin{aligned} \|v - \mathfrak{I}_h v\|_{0,K} &\leq ch_K |v|_{1,\omega_K}, \\ \|v - \mathfrak{I}_h v\|_{0,E} &\leq ch_E^{1/2} |v|_{1,\omega_E}, \end{aligned}$$

where the constant $c > 0$ depends only on the regularity parameters α_0 and c_1 , see Definition 1.

In the following, c denotes a generic constant that only depends on the parameters α_0 and c_1 from Definition 1. To state some properties of the regular mesh \mathcal{K}_h , we introduce the diameter h_{ω_z} of the neighbourhood ω_z .

Lemma 1. *Let \mathcal{K}_h be regular. Then, the mesh fulfils:*

1. *The number of nodes per element is uniformly bounded, i.e. $|\mathcal{N}(K)| \leq c$, $\forall K \in \mathcal{K}_h$.*
2. *Every node belongs to finitely many elements, i.e. $|\{K' \in \mathcal{K}_h : z \in K'\}| \leq c$, $\forall z \in \mathcal{N}_h$.*
3. *For all $z \in \mathcal{N}_h$ and $K \subset \omega_z$, it is $h_{\omega_z} \leq ch_K$.*

Proof. 1. Let $K \in \mathcal{K}_h$. In two dimensions, the number of nodes $|\mathcal{N}(K)|$ and the number of edges of the element K are identical. Since K is convex and since it lies in a square with side length h_K , the circumference $|\partial K|$ can be estimated in terms of h_K . Namely, it is $|\partial K| \leq 4h_K$. Additionally, we have $h_K \leq c_1 h_E$ for every edge E of K because of the regularity of \mathcal{K}_h . These facts yield

$$|\mathcal{N}(K)|h_K \leq c_1 \sum_{E \subset \partial K} h_E = c_1 |\partial K| \leq 4c_1 h_K$$

and prove the first part.

2. This follows by the fact, that every interior angle of an element is bounded from below by α_0 , due to the regularity of \mathcal{K}_h . Therefore, we have

$$|\{K' \in \mathcal{K}_h : z \in K'\}| \leq \left\lfloor \frac{2\pi}{\alpha_0} \right\rfloor,$$

where the term on the right denotes the biggest integer smaller than $2\pi/\alpha_0$.

3. We first recognise, that we have $h_{K'} \leq c_1 h_E \leq c_1 h_K$ for $K, K' \in \mathcal{K}_h$ with $E \subset K \cap K'$. If we apply this inequality successively in the neighbourhood ω_z of the node $z \in \mathcal{N}_h$, we obtain with \mathcal{Q} .

$$h_{K'} \leq c_1^{\lfloor 2\pi/\alpha_0 \rfloor - 1} h_K \quad \text{for arbitrary } K, K' \subset \omega_z.$$

This yields

$$h_{\omega_z} \leq 2 \max_{K' \subset \omega_z} h_{K'} \leq 2c_1^{\lfloor 2\pi/\alpha_0 \rfloor - 1} h_K \quad \text{for } K \subset \omega_z$$

and concludes the proof. □

Next, we show an approximation estimate for the L_2 -projection on patches. The important fact is here that the constant appearing in the estimate only depends on the regularity parameters of the mesh.

Lemma 2. *For every $z \in \mathcal{N}_h$ and $v \in H^1(\omega_z)$, we have*

$$\|v - Q_z v\|_{0, \omega_z} \leq ch_{\omega_z} |v|_{1, \omega_z}.$$

If $K \in \mathcal{K}_h$ with $K \subset \omega_z$, it follows

$$\|v - Q_z v\|_{0, \omega_z} \leq ch_K |v|_{1, \omega_z}.$$

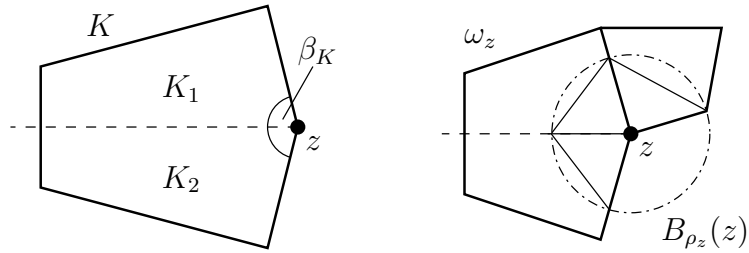


Figure 4: Element K which is split along the bisector of the angle β_K (left), patch ω_z with admissible decomposition $\{\omega_i\}_{i=1}^3$ and triangulation (right)

Proof. It is known that the first inequality holds with the Poincaré constant

$$C_P(\omega_z) = \sup_{v \in H^1(\omega_z)} \frac{\|v - Q_z v\|_{0,\omega_z}}{h_{\omega_z} |v|_{1,\omega_z}} < \infty,$$

see for example [17]. This constant depends only on the patch ω_z . Therefore, we have to show that the Poincaré constant $C_P(\omega_z)$ can be bounded independently of $z \in \mathcal{N}_h$ from above in terms of the regularity parameter α_0 and c_1 . For convex domains ω , Payne and Weinberger [14] showed $C_P(\omega) \leq 1/\pi$. In general, the patches ω_z are not convex, but they are star shaped with respect to z .

We distinguish two cases. First, we assume $\omega_z = K$ which is the trivial case. Since the element K is convex, we have $C_P(\omega_z) \leq 1/\pi \leq c$. If ω_z contains more than one element, we use Proposition 2.10 (Decomposition) of [17]. As preliminary of this Proposition, an admissible decomposition $\{\omega_i\}_{i=1}^n$ of ω_z with pairwise disjoint domains ω_i and $\bar{\omega}_z = \bigcup_{i=1}^n \bar{\omega}_i$ is needed. Admissible means here, that there exist triangles $\{T_i\}_{i=1}^n$ such that $T_i \subset \omega_i$ and for every pair i, j of different indices, there is a sequence $i = k_0, \dots, k_\ell = j$ of indices such that for every m the triangles $T_{k_{m-1}}$ and T_{k_m} share a complete side.

Let us construct a decomposition $\{\omega_i\}_{i=1}^n$ of ω_z which is admissible. For $z \in \mathcal{N}_h$, it is $\omega_z = \bigcup_{z \in K} K$. The angle between two neighbouring sides in a polygon K , which also might be labelled T_i or ω_i in the case of a triangle or a domain, at the node z is called β_K , see Figure 4. The set $\{\omega_i\}_{i=1}^n$ is defined as follows. It contains all elements $K \in \mathcal{K}_h$ with $z \in K$ which satisfy $\beta_K \leq \pi/2$. Additionally, if $\beta_K > \pi/2$ the set contains the two segments K_1 and K_2 which are obtained by splitting K along the bisector of the angle β_K , see again Figure 4. Due to the convexity of K , the segments K_1 and K_2 are also convex. We have constructed a decomposition $\{\omega_i\}_{i=1}^n$ of ω_z which satisfies $\alpha_0 \leq \beta_{\omega_i} \leq \pi/2$ for $i = 1, \dots, n$, where all ω_i are convex. According to Lemma 1, it is

$$n \leq 2|\{K \in \mathcal{K}_h : z \in K\}| \leq c.$$

In the next step, we intersect the boundary of the circle $B_{\rho_z}(z)$ with radius

$$\rho_z = \min \left\{ \inf_{x \in \partial\omega_z \setminus \Gamma} |z - x|, \min\{|z - x| : x \in \mathcal{N}_{h,D} \cup \mathcal{N}_{h,N}, x \in \partial\omega_z\} \right\}$$

centred in z with the edges of ω_i , $i = 1, \dots, n$ adjacent to z . The radius ρ_z is chosen in such a way that $\omega_i \cap B_{\rho_z}(z)$ for $i = 1, \dots, n$ is a circular sector. Afterwards, we connect the points of intersection in a way that we obtain a coarse triangulation $\{T_i\}_{i=1}^n$ of $\omega_z \cap B_{\rho_z}(z)$ with $T_i \subset \omega_i$ for $i = 1, \dots, n$, see Figure 4. According to the construction, every T_i is an isosceles triangle with angle $\beta_{T_i} = \beta_{\omega_i}$ at z which is enclosed by two sides of length ρ_z . Consequently, we have

$$|T_i| = \frac{1}{2}\rho_z^2 \sin \beta_{T_i} \geq \frac{1}{2}\rho_z^2 \sin \alpha_0 \quad \text{for } i = 1, \dots, n$$

and the diameter h_{T_i} of T_i fulfils

$$h_{T_i} = \max \left\{ \rho_z, 2\rho_z \sin \frac{\beta_{T_i}}{2} \right\} \leq 2\rho_z.$$

Obviously, the decomposition $\{\omega_i\}_{i=1}^n$ of ω_z is admissible. Thus, we can apply Proposition 2.10 (Decomposition) of [17] which yields

$$C_P(\omega_z) \leq \max_{1 \leq i \leq n} \left\{ 8(n-1) \left(1 - \min_{1 \leq j \leq n} \frac{|\omega_j|}{|\omega_z|} \right) (C_P^2(T_i) + 2C_P(T_i)) \frac{|\omega_z| h_{T_i}^2}{|T_i| h_{\omega_z}^2} \right\}^{1/2}$$

for the Poincaré constant. Since $|\omega_z| \leq h_{\omega_z}^2$, we obtain with the help of Lemma 1

$$\frac{|\omega_z| h_{T_i}^2}{|T_i| h_{\omega_z}^2} \leq \frac{h_{T_i}^2}{|T_i|} \leq \frac{4\rho_z^2}{\frac{1}{2}\rho_z^2 \sin \alpha_0} \leq \frac{8}{\sin \alpha_0} \leq c.$$

Therefore, we can bound $C_P(\omega_z)$ independently of $z \in \mathcal{N}_h$ in terms of α_0 and c_1 , i.e. $C_P(\omega_z) < c$.

The second inequality in the Lemma follows directly from the first one and Lemma 1. \square

Lemma 3. *Let $v \in H^1(K)$ and $E \subset \partial K$, then we have*

$$\|v\|_{0,E} \leq c \left\{ h_E^{-1/2} \|v\|_{0,T_E} + h_E^{1/2} |v|_{1,T_E} \right\}$$

with the isosceles triangle $T_E \subset K$ from the definition of regularity.

Proof. Let $\hat{T} = \{x \in \mathbb{R}^2 : 0 \leq x_i \leq 1, x_1 + x_2 \leq 1\}$ be the reference triangle with horizontal edge \hat{E} . According to the trace theorem, see e.g. [1], there exists a constant \hat{c} such that

$$\|\hat{v}\|_{0,\hat{E}} \leq \hat{c} \|\hat{v}\|_{1,\hat{T}}$$

for $\hat{v} \in H^1(\hat{T})$. Let $K \in \mathcal{K}_h$ be an arbitrary element with edge E and let $v \in H^1(K)$. Owing to the regularity of \mathcal{K}_h , there is a triangle $T_E \subset K$ with longest side E . We choose the affine transformation $F_{T_E} : \hat{T} \rightarrow T_E$ in such a way,

that \hat{E} is mapped onto E . We set $\hat{v} = v \circ F_{T_E} \in H^1(\hat{T})$. For this transformation it is known [5] that

$$|\hat{v}|_{m,\hat{T}} \leq C \|DF_{T_E}\|^m |\det DF_{T_E}|^{-1/2} |v|_{m,T_E} \quad \text{for } v \in H^m(T_E),$$

where C only depends on m and the spatial dimension which is equal to two here. Moreover, we have

$$\|DF_{T_E}\| \leq (2 + \sqrt{2})h_E \quad \text{and} \quad |\det DF_{T_E}| = 2|T_E| = \frac{1}{2} \tan(\alpha_0)h_E^2.$$

Using this transformation, we get

$$\begin{aligned} \|v\|_{0,E} &= h_E^{1/2} \|\hat{v}\|_{0,\hat{E}} \leq \hat{c} h_E^{1/2} \|\hat{v}\|_{1,\hat{T}} \\ &= \hat{c} h_E^{1/2} \left\{ \|\hat{v}\|_{0,\hat{T}}^2 + |\hat{v}|_{1,\hat{T}}^2 \right\}^{1/2} \leq \hat{c} h_E^{1/2} \left\{ \|\hat{v}\|_{0,\hat{T}} + |\hat{v}|_{1,\hat{T}} \right\} \\ &\leq c h_E^{1/2} \left\{ |\det DF_{T_E}|^{-1/2} \|v\|_{0,T_E} + |\det DF_{T_E}|^{-1/2} \|DF_{T_E}^{-1}\| |v|_{1,T_E} \right\} \\ &\leq c \left\{ h_E^{-1/2} \|v\|_{0,T} + h_E^{1/2} |v|_{1,T_E} \right\}. \end{aligned}$$

□

Finally, we can prove Proposition 1.

Proof. For $K \in \mathcal{K}_h$, we have

$$\sum_{z \in \mathcal{N}(K)} \psi_z = 1 \quad \text{in } K$$

and $\|\psi_z\|_{L^\infty(K)} = 1$ for $z \in \mathcal{N}(K)$. To prove the first estimate in the Proposition, we distinguish two cases. Let $K \in \mathcal{K}_h$ and let all nodes $z \in \mathcal{N}(K)$ of the element K be located in the interior of Ω or in the interior of the boundary Γ_N . Using Lemma 2, we obtain

$$\begin{aligned} \|v - \mathfrak{I}_h v\|_{0,K} &\leq \sum_{z \in \mathcal{N}(K)} \|\psi_z(v - Q_z v)\|_{0,K} \\ &\leq \sum_{z \in \mathcal{N}(K)} \|v - Q_z v\|_{0,\omega_z} \\ &\leq \sum_{z \in \mathcal{N}(K)} c h_K |v|_{1,\omega_z} \\ &\leq c h_K |v|_{1,\omega_K}. \end{aligned}$$

The last estimate is valid because of the fact that the number of nodes in $\mathcal{N}(K)$ is uniformly bounded with respect to $K \in \mathcal{K}_h$.

In the case that at least one node of the element K is on the boundary Γ_D , we write

$$\begin{aligned} v - \mathfrak{I}_h v &= \sum_{z \in \mathcal{N}(K)} \psi_z v - \sum_{z \in \mathcal{N}(K) \setminus \mathcal{N}_{h,D}} \psi_z Q_z v \\ &= \sum_{z \in \mathcal{N}(K)} \psi_z (v - Q_z v) + \sum_{z \in \mathcal{N}(K) \cap \mathcal{N}_{h,D}} \psi_z Q_z v \end{aligned}$$

and obtain

$$\|v - \mathfrak{I}_h v\|_{0,K} \leq \sum_{z \in \mathcal{N}(K)} \|\psi_z (v - Q_z v)\|_{0,K} + \sum_{z \in \mathcal{N}(K) \cap \mathcal{N}_{h,D}} \|\psi_z Q_z v\|_{0,K}.$$

The first sum has already been estimated, so let us have a look at the term in the second sum. For $z \in \mathcal{N}(K) \cap \mathcal{N}_{h,D}$, we have

$$\|\psi_z Q_z v\|_{0,K} \leq |Q_z v| \|\psi_z\|_{L^\infty(K)} |K|^{1/2} \leq h_K |Q_z v|.$$

Since $z \in \Gamma_D$, there is an element K' and an edge E' of K' such that $z \in E'$ and $E' \subset \Gamma_D$. Furthermore, there is an isosceles triangle $T_{E'}$ with $T_{E'} \subset K'$ due to the regularity of \mathcal{K}_h . Since v vanishes on E' , we obtain with Lemma 3 and $h_{E'}^{-1} \leq c_1 h_{K'}^{-1}$

$$\begin{aligned} |Q_z v| &= h_{E'}^{-1/2} \|Q_z v\|_{0,E'} = h_{E'}^{-1/2} \|v - Q_z v\|_{0,E'} \\ &\leq c h_{E'}^{-1/2} \left\{ h_{E'}^{-1/2} \|v - Q_z v\|_{0,T_{E'}} + h_{E'}^{1/2} |v - Q_z v|_{1,T_{E'}} \right\} \\ &\leq c \left\{ h_{K'}^{-1} \|v - Q_z v\|_{0,\omega_z} + |v|_{1,\omega_z} \right\}. \end{aligned}$$

Using Lemma 2 and putting all estimates together proves the first statement of Proposition 1.

To prove the second estimate in the Proposition, we proceed in a similar manner. Let $E \in \mathcal{E}_h$, we have

$$\sum_{z \in \mathcal{N}(E)} \psi_z = 1 \quad \text{on } E$$

and $\|\psi_z\|_{L^\infty(E)} = 1$ for $z \in \mathcal{N}(E)$. First, let $E \in \mathcal{E}_h$ such that all nodes z of the edge E are located in the interior of Ω or in the interior of the boundary Γ_N . Using Lemma 2 and 3 as well as $h_{K_E} h_E^{-1/2} \leq c_1 h_E^{1/2}$, where $K_E \in \mathcal{K}_h$ is an element

with edge E , we obtain

$$\begin{aligned}
\|v - \mathfrak{I}_h v\|_{0,E} &\leq \sum_{z \in \mathcal{N}(E)} \|\psi_z(v - Q_z v)\|_{0,E} \\
&\leq \sum_{z \in \mathcal{N}(E)} \|v - Q_z v\|_{0,E} \\
&\leq \sum_{z \in \mathcal{N}(E)} c \left\{ h_E^{-1/2} \|v - Q_z v\|_{0,T_E} + h_E^{1/2} |v - Q_z v|_{1,T_E} \right\} \\
&\leq \sum_{z \in \mathcal{N}(E)} c \left\{ h_E^{-1/2} \|v - Q_z v\|_{0,\omega_z} + h_E^{1/2} |v|_{1,\omega_z} \right\} \\
&\leq \sum_{z \in \mathcal{N}(E)} c h_E^{1/2} |v|_{1,\omega_z} \\
&\leq c h_E^{1/2} |v|_{1,\omega_E},
\end{aligned}$$

where T_E is the isosceles triangle of E with $T_E \subset K_E$.

If at least one node of E is on Γ_D , we have

$$\|v - \mathfrak{I}_h v\|_{0,E} \leq \sum_{z \in \mathcal{N}(E)} \|\psi_z(v - Q_z v)\|_{0,E} + \sum_{z \in \mathcal{N}(E) \cap \mathcal{N}_{h,D}} \|\psi_z Q_z v\|_{0,E}.$$

The first sum has already been estimated, so let us have a look at the term in the second sum. For $z \in \mathcal{N}(E) \cap \mathcal{N}_{h,D}$, we have

$$\|\psi_z Q_z v\|_{0,E} = |Q_z v| \|\psi_z\|_{0,E} = \frac{1}{\sqrt{3}} h_E^{1/2} |Q_z v|.$$

Since $z \in \Gamma_D$, there is an element K' and an edge E' of K' such that $z \in E'$ and $E' \subset \Gamma_D$. Furthermore, there is an isosceles triangle $T_{E'}$ with $T_{E'} \subset K'$ due to the regularity of \mathcal{K}_h . Since v vanishes on E' , we obtain with Lemma 3 and the condition $h_{E'}^{-1} \leq c_1 h_{K'}^{-1}$

$$\begin{aligned}
|Q_z v| &= h_{E'}^{-1/2} \|Q_z v\|_{0,E'} = h_{E'}^{-1/2} \|v - Q_z v\|_{0,E'} \\
&\leq c h_{E'}^{-1/2} \left\{ h_{E'}^{-1/2} \|v - Q_z v\|_{0,T_{E'}} + h_{E'}^{1/2} |v - Q_z v|_{1,T_{E'}} \right\} \\
&\leq c \left\{ h_{K'}^{-1} \|v - Q_z v\|_{0,\omega_z} + |v|_{1,\omega_z} \right\}.
\end{aligned}$$

Using Lemma 2 and putting all estimates together yields the second statement of Proposition 1 and concludes the proof. \square

5 Residual error estimate

In this section, we come to the main result. Among others, the residual error estimate measures the jumps of the conormal derivatives over the element edges.

This jump over an edge $E \in \mathcal{E}_h$ which lies in the interior of Ω is defined by

$$\llbracket u_h \rrbracket_E = a_K \gamma_1^K u_h + a_{K'} \gamma_1^{K'} u_h,$$

where $K, K' \in \mathcal{K}_h$ are the two neighbouring elements of E with $E \subset K \cap K'$. We assume that the Dirichlet boundary data g_D is approximated exactly, i.e. $g_{Dh} = g_D$. Consequently, it is possible to set $u_{Dh} = u_D$ and this yields $u - u_h \in H_D^1(\Omega)$.

Theorem 1. *Let \mathcal{K}_h be a regular mesh. Then the residual error estimate is reliable, i.e.*

$$|u - u_h|_{1,a,\Omega} \leq \frac{c}{\sqrt{a_{\min}}} \eta_R$$

with

$$\eta_R^2 = \sum_{K \in \mathcal{K}_h} \eta_K^2$$

and

$$\eta_K^2 = h_K^2 \|f\|_{0,K}^2 + \sum_{E \subset \partial K} h_E \|R_E\|_{0,E}^2,$$

where

$$R_E = \begin{cases} 0 & \text{for } E \subset \Gamma_D, \\ g_N - a_K \gamma_1^K u_h & \text{for } E \subset \Gamma_N \text{ with } E \subset \partial K, \\ -\frac{1}{2} \llbracket u_h \rrbracket_E & \text{else,} \end{cases}$$

and the constant $c > 0$ depends only on the regularity parameters α_0 and c_1 , see Definition 1.

Proof. In the first step, we define the functional ℓ on the dual of $H_D^1(\Omega)$ by

$$\begin{aligned} \ell(v) &= \int_{\Omega} a \nabla(u - u_h) \cdot \nabla v \, dx \\ &= \int_{\Omega} f v \, dx + \int_{\Gamma_N} g_N v \, ds_x - \sum_{K \in \mathcal{K}_h} \int_K a_K \nabla u_h \cdot \nabla v \, dx \\ &= \sum_{K \in \mathcal{K}_h} \int_K f v \, dx + \sum_{E \subset \Gamma_N} \int_E g_N v \, ds_x - \sum_{K \in \mathcal{K}_h} \int_{\partial K} a_K \gamma_1^K u_h v \, ds_x. \end{aligned}$$

If we rearrange the sums and take into account that we integrate over each edge in the interior of Ω two times, we obtain

$$\begin{aligned} \ell(v) &= \sum_{K \in \mathcal{K}_h} \left\{ \int_K f v \, dx + \sum_{E \subset \partial K \cap \Gamma_N} \int_E (g_N - a_K \gamma_1^K u_h) v \, ds_x \right. \\ &\quad \left. - \frac{1}{2} \sum_{E \subset \partial K \setminus \Gamma} \int_E \llbracket u_h \rrbracket_E v \, ds_x \right\} \\ &= \sum_{K \in \mathcal{K}_h} \left\{ \int_K f v \, dx + \sum_{E \subset \partial K} \int_E R_E v \, ds_x \right\}. \end{aligned}$$

The norm $\|\cdot\|_{1,\Omega}$ is equivalent to the semi norm $|\cdot|_{1,\Omega}$ on $H_D^1(\Omega)$ and it is also equivalent to the energy norm $|\cdot|_{1,a,\Omega}$ with

$$|w|_{1,a,\Omega}^2 = a_\Omega(w, w) = \int_{\Omega} a |\nabla w|^2 dx,$$

because of the assumption $0 < a_{\min} \leq a \leq a_{\max}$. Obviously, $H_D^1(\Omega)$ together with the weighted semi norm $|\cdot|_{1,a,\Omega}$ and the weighted scalar product $a_\Omega(\cdot, \cdot)$ is a Hilbert space. The functional ℓ belongs to the dual space of $H_D^1(\Omega)$ and so the theorem of Riesz yields $|u - u_h|_{1,a,\Omega} = \|\ell\|$. With the definition of the dual norm, we conclude

$$|u - u_h|_{1,a,\Omega} = \sup_{v \in H_D^1(\Omega)} \frac{|\ell(v)|}{|v|_{1,a,\Omega}}. \quad (5)$$

Next, we have to estimate $|\ell(v)|$. Using the Galerkin orthogonality

$$a_\Omega(u - u_h, v_h) = 0 \quad \text{for } v_h \in V_h,$$

the triangular inequality and Cauchy-Schwarz inequality, we obtain

$$\begin{aligned} |\ell(v)| &= |\ell(v - \mathfrak{I}_h v)| \\ &\leq \sum_{K \in \mathcal{K}_h} \left\{ \left| \int_K f(v - \mathfrak{I}_h v) dx \right| + \sum_{E \subset \partial K} \left| \int_E R_E(v - \mathfrak{I}_h v) ds_x \right| \right\} \\ &\leq \sum_{K \in \mathcal{K}_h} \left\{ \|f\|_{0,K} \|v - \mathfrak{I}_h v\|_{0,K} + \sum_{E \subset \partial K} \|R_E\|_{0,E} \|v - \mathfrak{I}_h v\|_{0,E} \right\}. \end{aligned}$$

The Cauchy-Schwarz inequality and the properties of the interpolation operator from section 4 yield

$$\begin{aligned} |\ell(v)| &\leq \sum_{K \in \mathcal{K}_h} \left\{ \|f\|_{0,K} ch_K |v|_{1,\omega_K} + \sum_{E \subset \partial K} \|R_E\|_{0,E} ch_E^{1/2} |v|_{1,\omega_E} \right\} \\ &\leq \frac{c}{\sqrt{a_{\min}}} \sum_{K \in \mathcal{K}_h} \left\{ h_K \|f\|_{0,K} |v|_{1,a,\omega_K} + \sum_{E \subset \partial K} h_E^{1/2} \|R_E\|_{0,E} |v|_{1,a,\omega_E} \right\} \\ &\leq \frac{c}{\sqrt{a_{\min}}} \sum_{K \in \mathcal{K}_h} \left\{ h_K \|f\|_{0,K} + \left(\sum_{E \subset \partial K} h_E \|R_E\|_{0,E}^2 \right)^{1/2} \right\} |v|_{1,a,\omega_K} \\ &\leq \frac{c}{\sqrt{a_{\min}}} \sum_{K \in \mathcal{K}_h} \left\{ h_K^2 \|f\|_{0,K}^2 + \sum_{E \subset \partial K} h_E \|R_E\|_{0,E}^2 \right\}^{1/2} |v|_{1,a,\omega_K} \\ &\leq \frac{c}{\sqrt{a_{\min}}} \left(\sum_{K \in \mathcal{K}_h} \eta_K^2 \right)^{1/2} |v|_{1,a,\Omega}. \end{aligned}$$

Applying (5) concludes the proof. \square

When the source function f in the differential equation is not known exactly and one has to approximate it with some function f_h , it is possible to extend the theorem in the usual way. In this case, the term $\|f - f_h\|_{0,\Omega}$ appears which is called data oscillation according to Morin, Nocketto and Siebert [13].

6 Implementation

An adaptive finite element method on polygonal meshes with hanging nodes and with the above introduced trial functions has been implemented.

In each iteration step of the adaptive scheme, we have to solve the boundary value problem on a given mesh. This means, that a system of linear equations has to be set up. As usual, the system matrix is assembled by local stiffness matrices. These local matrices are closely related to the symmetric discretization (3) of the local Steklov-Poincaré operators. In the case of a triangular mesh, the trial functions are exactly the hat functions which have piecewise linear Dirichlet and piecewise constant Neumann traces on each element. Due to the choice of the discretization in the BEM, we obtain the same global system matrix as for a standard FEM with linear trial functions apart from numerical errors.

A new procedure has been implemented to refine the polygonal meshes locally and globally. For the decision how to split an element K into two new ones, we first compute the matrix

$$M_{\text{Cov}} = \int_K (x - \bar{x})(x - \bar{x})^\top dx$$

where

$$\bar{x} = \frac{1}{|K|} \int_K x dx.$$

It is known that M_{Cov} is a symmetric positive definite two by two matrix. The eigenvector to the biggest eigenvalue points into the direction of the longest extend of the element K . Therefore, we split the element orthogonal to this eigenvector through the centre \bar{x} of K and obtain two new elements, see Figure 5. The regularity of the mesh has to be ensured by the implementation. Figures 6 and 11 show examples of such meshes and their refinements. Similar ideas are used in [15] to build up cluster trees for matrix approximation.

The adaptive strategy is as follows. The boundary value problem is solved on a mesh. Afterwards, the error indicators η_K for all $K \in \mathcal{K}_h$ are calculated and we mark some elements due to the Dörfler strategy [10]. Then, we refine the marked elements and obtain a new mesh. Now we can solve the problem again on the refined mesh. This loop can be repeated until the desired accuracy is achieved.

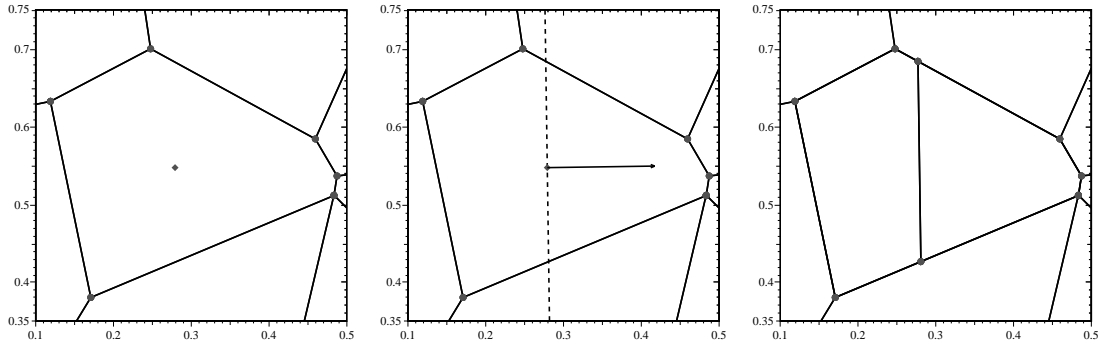


Figure 5: Refinement of an element: element with centre \bar{x} (left), element with eigenvector (middle), two new elements (right)

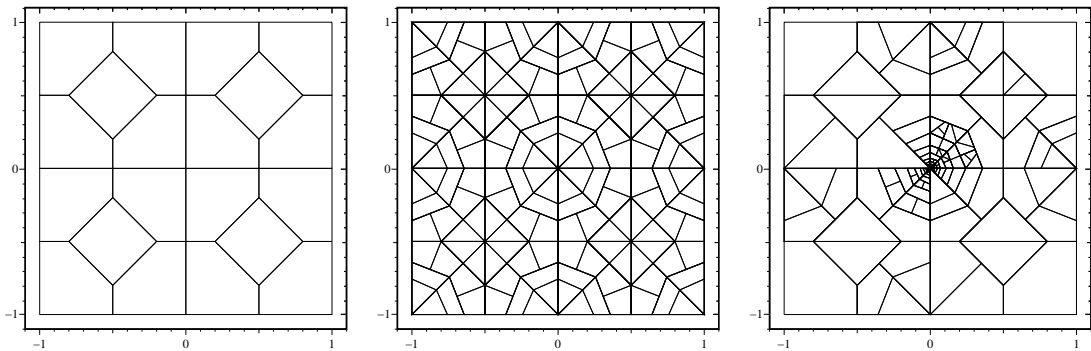


Figure 6: Initial mesh (left), uniform refined mesh (middle), adaptive refined mesh (right)

7 Numerical examples

In this section, we have a look at different numerical examples to confirm our theoretical results. Let $\Omega = (-1, 1) \times (-1, 1) \subset \mathbb{R}^2$ be split into two domains, $\Omega_1 = \Omega \setminus \overline{\Omega}_2$ and $\Omega_2 = (0, 1) \times (0, 1)$. We are interested in the boundary value problem

$$\begin{aligned} -\operatorname{div}(a(x)\nabla u(x)) &= 0 && \text{for } x \in \Omega, \\ u(x) &= g(x) && \text{for } x \in \Gamma = \Gamma_D, \end{aligned}$$

where the coefficient a is given by

$$a(x) = \begin{cases} 1 & \text{for } x \in \Omega_1, \\ k_2 & \text{for } x \in \Omega_2. \end{cases}$$

Using polar coordinates (r, φ) , we choose the boundary data as restriction of the global function

$$g(x) = r^\lambda \begin{cases} \cos(\lambda(\varphi - \pi/4)) & \text{for } x \in \overline{\Omega}_2, \\ \beta \cos(\lambda(\pi - |\varphi - \pi/4|)) & \text{else,} \end{cases}$$

with

$$\lambda = \frac{4}{\pi} \arctan \left(\sqrt{\frac{3+k_2}{1+3k_2}} \right) \quad \text{and} \quad \beta = -k_2 \frac{\sin\left(\lambda \frac{\pi}{4}\right)}{\sin\left(\lambda \frac{3\pi}{4}\right)}.$$

This problem is constructed in such a way that $u = g$ is the exact solution in Ω . The parameter $k_2 > 0$ is responsible for the regularity of the solution. If $k_2 < 1$ we have $u \in H^2(\Omega)$ and otherwise u is singular in the sense that the gradient of u is not squared integrable any more. Figure 7 displays approximations of the function g for two different values of k_2 .

When the solution of the problem fulfils $u \in H^2(\Omega)$, it is known that the finite element method with linear trial functions on admissible meshes converges quadratically in the mesh size h with respect to the L_2 -norm on uniform refined meshes. If we sketch the approximation error $\|u - u_h\|_{0,\Omega}$ with respect to the degrees of freedom (DoF) in a logarithmic plot we expect a slope of one, since $h = O((\text{DoF})^{-1/2})$. This behaviour is shown in the first numerical example for the introduced finite element method. We choose $k_2 = 0.01$ so that $u \in H^2(\Omega)$ and start with a polygonal mesh (see Figure 6). In every iteration step we refine all elements and hanging nodes appear naturally. In Figure 8, we can recognise quadratic convergence for the proposed method on arbitrary polygonal meshes with hanging nodes.

In the next numerical experiment we are going to examine the rate of convergence with respect to the energy norm $|\cdot|_{1,a,\Omega}$. We perform the adaptive strategy with the error estimate η_R and the method with uniform refinement. From the theory of standard finite element methods, we would expect linear convergence for the

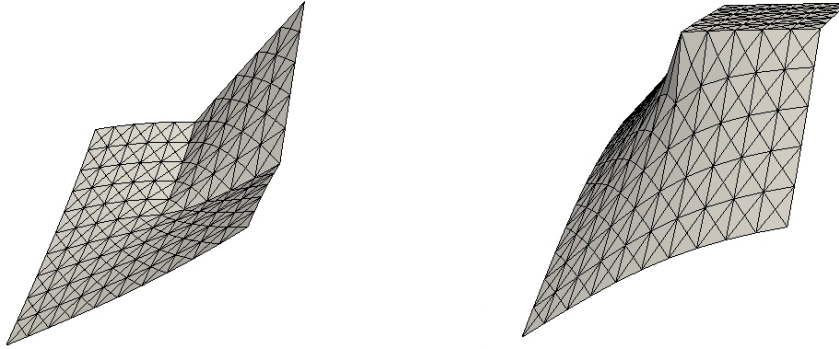


Figure 7: $k_2 = 0.01$ and therefore $g \in H^2(\Omega)$ (left), $k_2 = 100$ and so $g \notin H^2(\Omega)$ (right)

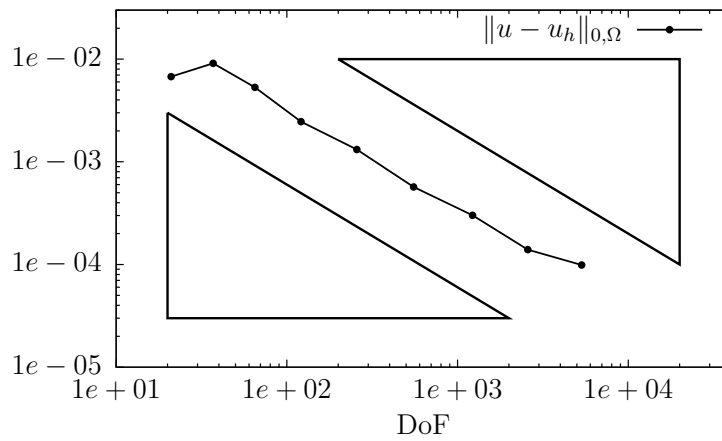


Figure 8: Convergence for smooth solution ($k_2 = 0.01$) using uniform refinement, triangles with slope one

uniform strategy. Indeed, we observe linear convergence for the uniform and for the adaptive strategy with the proposed method (see Figure 9). We can also recognise that the error estimate η_R reproduces the behaviour of the error $|u - u_h|_{1,a,\Omega}$ asymptotically very well.

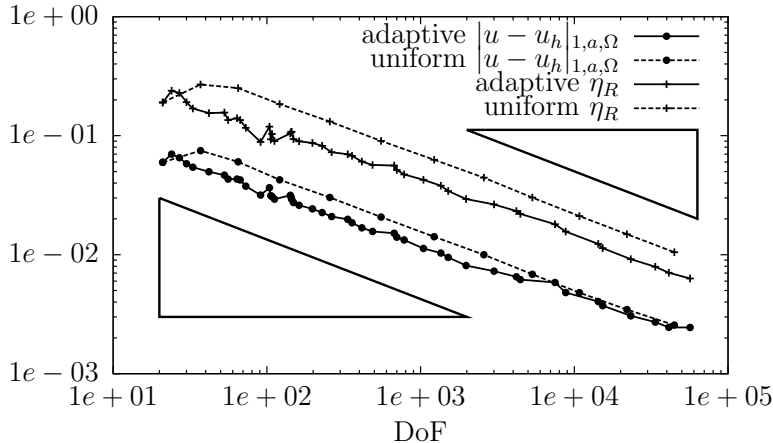


Figure 9: Convergence for smooth solution ($k_2 = 0.01$) using adaptive and uniform refinement, triangles with slope one half

If one considers boundary value problems with smooth solutions it is very difficult for an adaptive strategy to perform better than an uniform one. Therefore, we want to choose the problem in such a way that it has a singular solution. For $k_2 = 100$, we obtain the convergence results shown in Figure 10. Obviously, the error stays more or less constant at the beginning of the two strategies. This can be explained as follows. In our considerations, we have assumed that the boundary data is approximated exactly but this assumption is not true here. The error in the Dirichlet data dominates. Consequently, the method needs some refinement steps until the data is approximated accurately enough to perform well. Nevertheless, we can see that the rate of convergence for the uniform refinement slows down. In contrast, the adaptive method still converges linearly.

Finally, a standard example is considered. We use again the polar coordinates (r, φ) . Let $\Omega = \{x \in \mathbb{R}^2 : |r| < 1 \text{ and } 0 < \varphi < 3\pi/2\}$ and

$$g(x) = r^{2/3} \sin\left(\frac{2\varphi}{3}\right) \quad \text{for } x \in \mathbb{R}^2.$$

The problem reads

$$\begin{aligned} -\Delta u(x) &= 0 & \text{for } x \in \Omega, \\ u(x) &= g(x) & \text{for } x \in \Gamma = \Gamma_D. \end{aligned}$$

It looks very simple but the solution $u = g$ is singular in the origin. In Figure 11, you can see the initial mesh and two adaptive refinements after five and ten

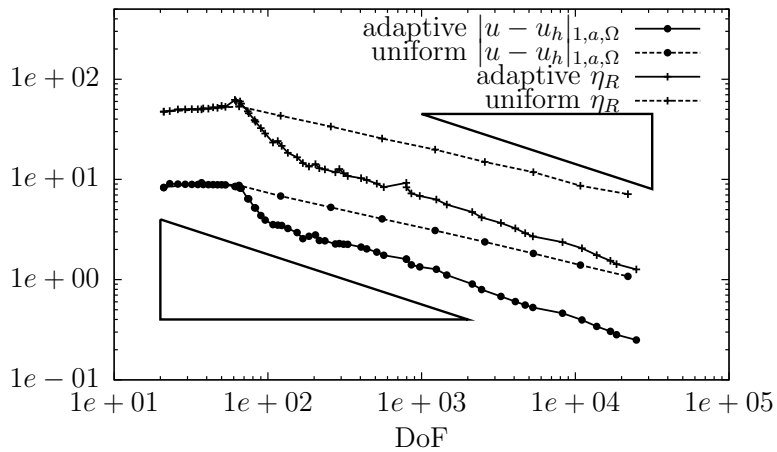


Figure 10: Convergence for singular solution ($k_2 = 100$) using adaptive and uniform refinement, triangles with slope one half

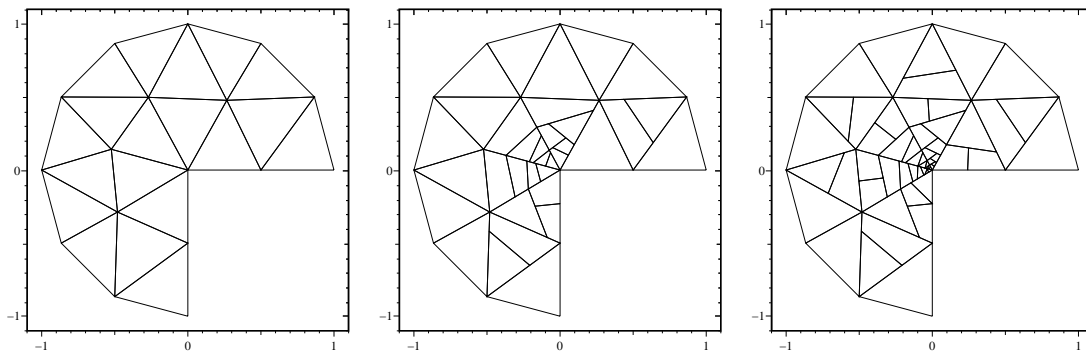


Figure 11: Initial mesh (left), adaptive refined mesh after five steps (middle), adaptive refined mesh after ten steps (right)

steps. The adaptive finite element method obviously recognises the singularity and refines the mesh near the origin. Typically, one would expect that all elements near the origin should be refined in a similar manner. But in Figure 11, the triangle on the upper right of the origin is still not refined after five steps. Even after ten steps, there are big elements near the origin. This is a difference to standard finite element methods, where values at hanging nodes are obtained by interpolation of values at classical nodes. In the proposed BEM-based FEM, a hanging node gives a degree of freedom and adds a trial function to the approximation space V_h . These trial functions also affect the approximation quality at neighbouring elements. In Figure 12, we can see that the error over the upper right triangle of the origin is reduced by introducing hanging nodes without refining the element.

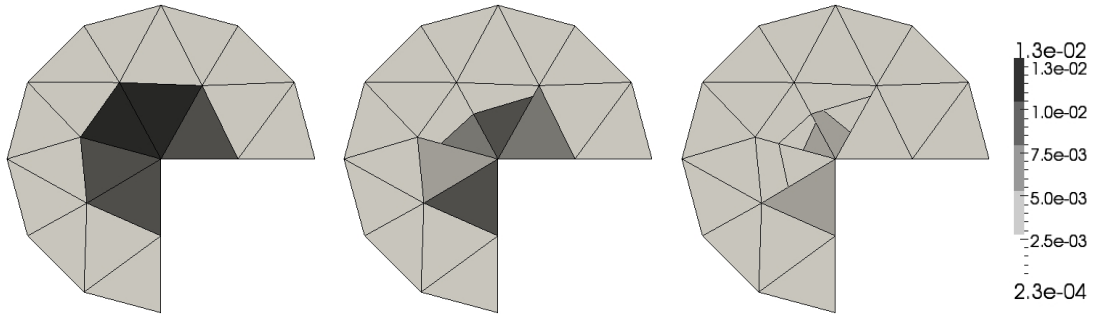


Figure 12: Error distribution $\|u - u_h\|_{1,a,K}^2$ for the first three meshes

The convergence analyses for this example shows the same results as in the last example. The uniform method does not converge linearly any more but the adaptive strategy has still linear convergence (see Figure 13).

8 Conclusions

The proposed method can be seen as a generalisation of standard finite element methods, since these two methods are equivalent on triangular and quadrilateral meshes. Actually, the BEM-based FEM has the advantage that it works on arbitrary polygonal meshes with convex elements and it handles hanging nodes in a natural way. To the best of our knowledge, the present paper contains the first a posteriori error estimate for the BEM-based FEM. In industrial applications, this allows us to check the accuracy of the approximation in a region of special interest if only one mesh is available without refinements. Therefore, we can judge the quality of the mesh and optimize it if necessary. Additionally, we can perform adaptive finite element strategies and yield optimal convergence.

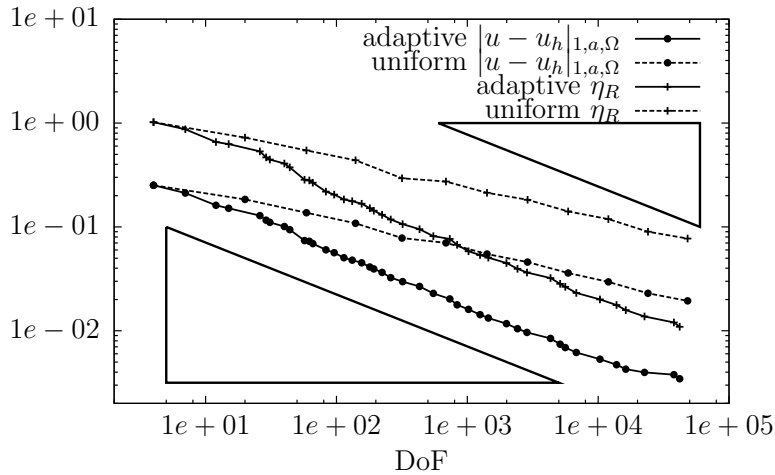


Figure 13: Convergence for singular solution on arc, triangles with slope one half

9 Acknowledgement

This paper is first published in the journal *Numerische Mathematik*, see [19]. The final publication is available at www.springerlink.com.

References

- [1] R. A. Adams. *Sobolev Spaces*. Academic Press, 1975.
- [2] R. Becker, P. Hansbo, and M.G. Larson. Energy norm a posteriori error estimation for discontinuous Galerkin methods. *Computer Methods in Applied Mechanics and Engineering*, 192(5-6):723–733, 2003.
- [3] L. Beirao da Veiga. A residual based error estimator for the mimetic finite difference method. *Numerische Mathematik*, 108(3):387–406, 2008.
- [4] F. Brezzi, K. Lipnikov, and M. Shashkov. Convergence of the mimetic finite difference method for diffusion problems on polyhedral meshes. *SIAM J. Numer. Anal.*, 43(5):1872–1896 (electronic), 2005.
- [5] P. G. Ciarlet. *The Finite Element Method for Elliptic Problems*. North-Holland, Amsterdam, 1978.
- [6] Ph. Clément. Approximation by finite element functions using local regularization. *Rev. Française Automat. Informat. Recherche Opérationnelle Sér. RAIRO Analyse Numérique*, 9(R-2):77–84, 1975.
- [7] D. Copeland, U. Langer, and D. Pusch. From the boundary element domain decomposition methods to local Trefftz finite element methods on polyhedral

- meshes. *Domain Decomposition Methods in Science and Engineering XVIII*, pages 315–322, 2009.
- [8] D.M. Copeland. Boundary-element-based finite element methods for Helmholtz and Maxwell equations on general polyhedral meshes. *Int. J. Appl. Math. Comput. Sci.*, 5(1):60–73, 2009.
- [9] V. Dolejší, M. Feistauer, and V. Sobotíková. Analysis of the discontinuous Galerkin method for nonlinear convection-diffusion problems. *Comput. Methods Appl. Mech. Engrg.*, 194(25-26):2709–2733, 2005.
- [10] W. Dörfler. A convergent adaptive algorithm for Poisson’s equation. *SIAM J. Numer. Anal.*, 33(3):1106–1124, 1996.
- [11] C. Hofreither, U. Langer, and C. Pechstein. Analysis of a non-standard finite element method based on boundary integral operators. *Electronic Transactions on Numerical Analysis (ETNA)*, 37:413–436, 2010.
- [12] W.C.H. McLean. *Strongly elliptic systems and boundary integral equations*. Cambridge Univ Pr, 2000.
- [13] P. Morin, R.H. Nochetto, and K.G. Siebert. Data oscillation and convergence of adaptive FEM. *SIAM Journal on Numerical Analysis*, 38(2):466–488, 2001.
- [14] L. E. Payne and H. F. Weinberger. An optimal Poincaré inequality for convex domains. *Arch. Rational Mech. Anal.*, 5:286–292, 1960.
- [15] S. Rjasanow and O. Steinbach. *The fast solution of boundary integral equations*. Mathematical and analytical techniques with applications to engineering. Springer, 2007.
- [16] O. Steinbach. *Numerical approximation methods for elliptic boundary value problems: finite and boundary elements*. Springer, 2007.
- [17] A. Veiser and R. Verfürth. Poincaré constants of finite element stars. *IMA J. Numer. Anal.*, 2010. (Accepted).
- [18] R. Verfürth. *A review of a posteriori error estimation and adaptive mesh-refinement techniques*. Wiley-Teubner, 1996.
- [19] S. Weißer. Residual error estimate for BEM-based FEM on polygonal meshes. *Numerische Mathematik*, 118:765–788, 2011. 10.1007/s00211-011-0371-6.
- [20] E. Wienholtz, H. Kalf, and T. Kriecherbauer. *Elliptische Differentialgleichungen zweiter Ordnung*. Springer-Verlag, Berlin Heidelberg, 2009.